Supporting Information for

Orientational nanoconjugation with gold endows markedly antimicrobial potentials and drugability of ultra-short dipeptides

Zhiye Zhang[1,¶], Yaoyao Chen[2,¶], Jinai Gao[1,3,¶], Min Yang[1,8¶], Dengdeng Zhang[1,4], Le Wang[5], Tianyu Zhang[6], Qiqi Cao[2], James Mwangi[1,8], Chenglu He[7], Ya Li[7], Xiangsheng Liu[6], Xingyu Jiang[5], Peter Muiruri Kamau[1,8], Ren Lai[1,3]*

[1]Engineering Laboratory of Peptides of Chinese Academy of Sciences, Key Laboratory of Bioactive Peptides of Yunnan Province, KIZ-CUHK Joint Laboratory of Bioresources and Molecular Research in Common Diseases, National Resource Center for Non-Human Primates, National Research Facility for Phenotypic & Genetic Analysis of Model Animals (Primate Facility), and Sino-African Joint Research Center, New Cornerstone Science Institute, Kunming Institute of Zoology, Chinese Academy of Sciences, Kunming, Yunnan 650223, China;

[2]Department of Zoology, College of Life Sciences, Nanjing Agricultural University, Nanjing 210095, Jiangsu, China;

[3]School of Molecular Medicine, Hangzhou Institute for Advanced Study, University of Chinese Academy of Sciences, Hangzhou 310024, Zhejiang, China;

[4]Department of Pharmaceutical Sciences, College of Pharmaceutical Sciences, Soochow University, Suzhou 215123, Jiangsu, China;

[5]Department of Biomedical Engineering, Southern University of Science and Technology, Shenzhen 518055, Guangdong, China;

[6]Zhejiang Cancer Hospital, Hangzhou Institute of Medicine (HIM), Chinese Academy of Sciences, Hangzhou 310022, Zhejiang, China;

[7]Department of Clinical Laboratory, First Affiliated Hospital of Kunming Medical College, Kunming 650032, Yunnan, China.

[8]Kunming College of Life Science, University of Chinese Academy of Sciences, Kunming 650204, Yunnan, China;

¶These authors contributed equally to this work.

Author to whom correspondence should be addressed to R.L. (rlai@mail.kiz.ac.cn).

Supporting Information include:

Additional experimental details

Supplementary Figure S1-S8

Supplementary Table S1-S3

Supplementary References

Additional experimental details

Materials

$HAuCl_4 \cdot 3H_2O$ was purchased from Sigma (USA). Other chemicals and solvents were from Solarbio (China). The short peptides were synthesized by GL Biochem Ltd. (Shanghai, China) with their purities > 98%, determined by reversed-phase high-performance liquid chromatography (RP-HPLC) and mass spectrometry.

Synthesis of short peptide-gold nanoparticles

Each short peptide solution (10 mM dissolved in 10 mL of methanol, 200 μL of absolute acetic acid, and 80 μL of Tween-80) was first mixed with $HAuCl_4$ solution (5 mM in 20 mL of methanol) for 10 min in an ice-water bath, followed by the dropwise addition of $NaBH_4$ solution (60 mM in 5 mL of methanol) with vigorous stirring. The mixture was continuously stirred at a low speed for an additional 1 h. Methanol was removed by freeze-drying and 5 mL of deionized water was then added to the residue, followed by dialysis (14 kDa MW cutoff, Millipore) with deionized water for 48 h to remove unreacted peptide and buffer ions. The samples were sterilized using a 0.22-μm filter (Millipore, USA) and then stored at 4 °C for further use. The modified nanoparticles (NPs) were well-dispersed and stable in aqueous solution at 4 °C for 6 months.

NP characterization

The concentrations of NPs were determined by measuring elemental gold with inductively coupled plasma analysis (ICP, Perkin-Elmer Optima 5300DV, USA). The ultraviolet visible (UV-vis) spectra of NPs were recorded using a microplate reader (synergy MX, BioTek, USA). Zeta potentials were measured by light scattering via Zetasizer Nano ZS (Malvern Company, England). X-ray photoelectron spectroscopy (XPS) was used to determine the Au:S ratio on the coated NPs. The number of gold

atoms and oligopeptides per NP were calculated according to our previously described methods[1]. Transmission electron microscopy (TEM) was carried out to characterize the morphologies of the gold NPs. A minimum of 100 NPs were measured using Image J software for particle size analysis.

Bacteria strain preparation and growth conditions

The *Escherichia coli* (25922), *Candida albicans* (SC5341), *Bacillus subtilis* and *Staphylococcus aureus* (ATCC2592 and 19 clinically isolated strains presented as 1184-1, 1184-2, 21441-1, 21441-2, 22081-1, 22082-2, 22082-3, 1519-1, 1519-2, 8310, 9431, 11268, 15775, 11, 31, 32, 51, 52, and Z) were obtained from the First Affiliated Hospital of Kunming Medical University, Yunnan, China. Yeast peptone dextrose (YPD) medium (10 g/L yeast extract, 20 g/L peptone, and 20 g/L glucose) was used for routine growth of *C. albicans*. The other bacterial strains were cultured in Luria-Bertani (LB) broth.

Antimicrobial properties *in vitro*

The minimal inhibitory concentrations (MICs) of samples against all strains of bacteria were determined using the tube microdilution assay according to our previously described methods[2]. MIC was defined as the lowest concentration of the test samples that resulted in no detectable bacterial growth.

Hemolysis and cytotoxicity assays

Human red blood cells was collected from healthy human volunteers and used for hemolysis assay, and human HaCaT keratinocyte cells and human umbilical vein endothelial cells (HUVECs) (cultured in Dulbecco's modified Eagle medium, DMEM, Gibco, Grand Island, NJ, USA) were used in the cytotoxicity assays. The hemolysis and cytotoxicity assays were determined based on our previously published procedures[2]. Hemolysis assay using human blood samples were approved by the

Institutional Review Board at the Kunming Institute of Zoology (KIZRKX-2021-XZ-003).

Bacterial killing kinetic assay

The bacterial killing kinetic assay was performed according to our previous method[2]. In brief, *S. aureus* ATCC2592 was first cultured to the exponential phase and diluted to 2×10^5 CFU/mL with fresh LB broth. Au_CR (1, 5, 10 × MIC) or vancomycin (1, 5, 10 × MIC) was the added to the bacterial suspension and incubated at 37 °C for 0, 1, 10, 30, 60, and 180 min, respectively. Aliquots (10 μL) were extracted at each time point and diluted (100 times) with fresh broth, with 100 μL of the dilution then seeded onto agar plates. After incubation at 37 °C for 24 h, viable colonies were determined.

Induction of resistance

Serial passages (24 h for one passage) were used to evaluate the development of resistance following long-term exposure to Au_CR or vancomycin. First, *S. aureus* ATCC2592 was cultured in LB broth with constant shaking at 160 rpm and 37 °C. The bacteria (20 μL) were transferred daily into 1 mL of fresh medium with or without the test samples. The concentration of test samples was initially used as 0.1 × MIC, and doubled after every 10 passages (i.e. 0.2, 0.4, 0.8, 1.6, 3.2 × MIC for 11-20, 21-30, 31-40, 41-50, and 51-60 passages, respectively). After every five passages, the bacterial suspension was stored at −20 °C. The MICs for resistant-induced, control, and original strains were assessed every five passages as described above.

Biofilm inhibition and eradication assays

Biofilm inhibition assays were performed as described previously[2]. Briefly, 200 μL of 1×10^6 CFU/mL *S. aureus* ATCC 2592 and Z (clinically isolated strain) were cultured with LB in 96-well plates at 37 °C for 24 h in the presence or absence of Au_CR (0.5–8 × MIC). At 24 h after incubation, the planktonic bacteria were

removed by washing with sterile PBS solution three times. Methanol (99%) was then added and fixed for 15 min. After aspiration, the plates were allowed to dry. Dried wells were stained with 100 μL of 0.1% crystal violet for 5 min, after which excess stain was gently rinsed off with tap water. The stain was resolubilized in 95% ethanol and absorbance was measured at 600 nm.

For the biofilm eradication assay, the *S. aureus* ATCC2592 and Z (clinically isolated strain) biofilms were first developed in 96-well plates at 37 °C for 24 h by adding 100 μL of bacteria (1×10^5 CFU/mL) to LB medium. After washing the wells three times with PBS, serial dilutions of Au_CR (0.5–8 × MIC) in 100 μL of LB medium were added (with 100 μL of sterile medium added as the negative control). The plates were then placed in a shaking incubator (100 rpm) at 37 °C for 24 h. After incubation, the wells were emptied and washed three times with 200 μL of PBS and air fixed for 1 h under aseptic conditions. The percentage of biofilm removal was quantified by measuring the absorbance after applying crystal violet stain as described above.

Antibacterial properties against persister cells

First, *S. aureus* ATCC2592 was cultured to the exponential phase and diluted to 1×10^8 CFU/mL with fresh LB broth. This suspension (100 μL) was then transferred to a 96-well plate and incubated at 37 °C for 24 h. The planktonic bacteria were removed by washing three times with sterile PBS, and 100 μL of fresh medium with vancomycin (50 × MIC) was then added to the wells, followed by incubation for an additional 24 h. The planktonic bacteria were again removed by washing three times with PBS, and the adherent persisters were then dislodged in 100 μL of fresh PBS by 5 min of sonication. Serial dilutions of Au_CR (0.5–8 × MIC) were added to the persister suspension and incubated at 37 °C for 12 h, after which time the number of

viable bacteria was determined microbiologically.

Evaluation of bacterial membrane permeabilization

The effects of Au_CR on the bacterial membrane were evaluated using TEM, scanning electron microscopy (SEM), fluorescence assay, and flow cytometry. TEM and SEM were performed to determine membrane morphology, as described in our previous research[1,2]. Briefly, *S. aureus* ATCC2592 was first cultured in LB broth to the exponential phase. After two washes with 0.15 M saline, the bacterial pellets were re-suspended and incubated with or without Au_CR (5 × MIC) at 37 °C for 30 min. The suspension was then centrifuged at 1 000 rpm at 4 °C for 10 min and the residual pellets were fixed with 2.5% buffered glutaraldehyde and 1% osmium tetroxide at 4 °C for 2 h. After dehydration, embedding, and staining, the sections were observed by TEM (JEOL, JEM-1011, Japan). Some slices were further stained with 2% uranyl acetate and 0.2% lead citrate, while others remained unstained. Some pellets were dehydrated in a graded series of ethanol, frozen in liquid nitrogen, cooled in tertbutyl alcohol, and vacuum dried overnight, followed by mounting onto aluminum stubs and vacuum sputter-coating with gold. Membrane morphology was observed with a Hitachi S-3000N (Japan) SEM.

For the fluorescence assay, mid-log phase *S. aureus* ATCC2592 culture was harvested by centrifugation at 3 500 rpm at 4 °C for 10 min. After washing with phosphate-buffered saline (PBS), the bacterial pellets were re-suspended in the same buffer at a dilution of 1×10^8 colony-forming units (CFU)/mL. The bacterial suspension was then treated with Au_CR (5 × MIC) at 37 °C for 30 min on a shaker bed at 200 rpm. The suspensions were centrifuged (3 500 rpm at 4 °C for 10 min) and the pellets were re-suspended in 1 mL PBS followed by the addition of propidium iodide (PI) (Sigma, USA) at a final concentration of 5 μg/mL for 30 min at room

temperature. The bacterial cells were then observed and imaged with an Olympus FluoView 1000 confocal microscope (Olympus, Melville, NY, USA).

For kinetics of PI staining, mid-log phase cultures of *S. aureus* ATCC2592 were diluted in PBS to 1×10^6 CFU/mL. The bacteria suspension was then incubated for 15 min on ice in the dark with PI dye at a final concentration of 10 μg/mL. After incubation, PI fluorescence was measured over time via flow cytometry (BD LSRFORTESAA™, USA). Controls bacteria were exposed to PBS without Au_CR, while test bacteria were treated with Au_CR (5 × MIC). Samples fluorescence was measured immediately over 6 min.

Membrane potential measurement

We used the fluorescent dye 3,3-dipropylthiadicarbocyanine iodide ($DiSC_3(5)$) to evaluate the changes of membrane potential as previously described[3]. Briefly, *S. aureus* ATCC2592 cells were harvested from exponential phase cultures and suspended in sterile saline (0.9%) containing 100 mM KCl, diluted to 2×10^5 CFU/mL with fresh LB broth. The bacterial suspension was then adjusted to an OD600 of 0.1, followed by adding $DiSC_3(5)$ to reach a final concentration of 0.5 μM. The cell suspension (190 μL) was then added to the wells of a 96-well plate (black wall, clear bottom, Greiner Bio-One). Once the DiSC3(5) signal had reduced to close to zero, the samples (Au_CR (1–8 × MIC), Nisin A (4 μM), and Valinomycin (10 μM), 10 μL) were added to the wells. Saline was used as control. Fluorescence was measured at an excitation wavelength of 622 nm and emission wavelength of 670 nm, with the BioTek Synergy H1 plate reader (BioTek Instruments, Inc. USA). Three biological repeats were performed.

Simulation setup

The molecular dynamic (MD) simulations were performed with GROMACS 2021.5 package[4] using Martini 2.0 force field[5]. The initial atomistic Au_CR structure with a core size of 3 nm was retrieved from the combination use of Nanoparticle Builder Module in OpenMD[6] and Packmol[7] software. The 3 nm gold core was cut from a face-centered cubic (FCC) gold lattice structure with a lattice parameter of 4.08 Å[8]. The CR peptide unit was built as short linear peptides. In accordance with Supplemental Table S1, high ratio CR peptides with number of 383 was conjugated to the gold core by constraining the position of S atoms in cysteine residues, distributing around the gold core for ensuring Au-S bonding. The longer side chain of arginine toward the outside direction undertake the main charge properties of the particle. All gold atoms were mapped to a C1 bead. The peptides were converted to coarse-grained (CG) beads by the martinize.py tool using Martini 2.0 force filed parameters. Because the gold core was completely wrapped by the peptides, it was seen only as a carrier without participating the interaction with membrane. The Lennard-Jones (LJ) parameters of gold atoms were taken from the paper of Heinz et al[9,10]. To maintain the spherical geometry, all Au-S bonds were constrained with a harmonic bonding potential of K_b=1250 kJ mol^{-1} nm^{-2}. A complex membrane consisting 1,2-dioleoyl-sn-glycerol-3-phosphocholine (DOPC) and 1, 2-dioleoyl-sn-glycero-3-phospho-(1'-rac-glycerol) (DOPG) with a ratio of 7:3 was considered to represent the bacterial membrane model, especially to simulate negatively charged *S. aureus* membranes[11,12]. The initial membrane was constructed using the INSANE building tool[13], which is a useful tool to generate membrane configuration in Martini force field. The CG model of phospholipids was obtained from the previous study of Marrink et al[14].The initial periodic box was created with a dimension of 20 nm×20 nm×20 nm. The membrane was placed in the center of the

box and Au_CR particle was placed in a 7 nm distance above the membrane center in one side. The counter ions were also added to neutralize the system.

At first, to remove the bad contacts between beads, the system was minimized using the steepest descent algorithm and subsequently a 0.5 μs equilibration process. The v-rescale[15] and Berendsen algorithms[16] were used for temperature and pressure control in equilibration runs, respectively. Then, the production simulations performed. A 1.1 nm cutoff was used for van der Waals (vdW) interactions. A particle mesh Ewald (PME) method[17] was used to deal with the long range Coulombic interactions. The periodic boundary condition was set to x, y, z directions. All the production runs were performed using a v-rescale thermostat[15] at 310 K for temperature, while the pressure coupling was controlled with a Parrinello-Rahman algorithm[18] . A semi-isotropic scaling method setup at 1 bar and a compressibility of pressure was set to $\beta = 4.5 \times 10^{-5}$ bar^{-1}. The simulation was performed 30 μs with a time step of 20 fs. The trajectory of production runs was used for analysis by GROMACS tools. The software VMD[19] and Pymol[20] were used for structure visualization and figure making.

Liposome leakage assay

Biomembrane-mimicking unilamellar vesicles were prepared as a previously described method[21]. Briefly, DOPC and DOPG stock solutions at a mass ratio of 7:3 were mixed with 1,2-dipalmitoyl-sn-glycero-3-phosphoethanolamine-N-(capbiotinyl) (Biotinyl-cap PE, 0.1 mol%) and DiI (0.02 mol%). The resulting mixtures were dried under N_2, desiccated under vacuum for 2 h. Phosphate buffer containing Fluo-4 (at 25 μg/mL) was added to the lipid film for lipid rehydration to form Fluo-4 encapsulated liposomes to achieve a lipid concentration of 2 mg/mL. The resulting solutions were sonicated to clarity and extruded through a polycarbonate filter with 400 nm pore size

(GE Healthcare) using a mini-extruder (Avanti Polar Lipids) to form homogenous unilamellar vesicles.

The liposomes were immobilized on a coverslip via biotin-streptavidin interaction. Phosphate buffer containing Ca^{2+} (at 10 μM) and Au_CR (5 × MIC) was added in situ, and images were captured after 0, 10, and 30 min of incubation in both the Fluo-4 and DiI channels with an Olympus FluoView 1000 confocal microscope (Olympus, Melville, NY, USA). The percentage of the permeabilized liposomes was calculated using Image J software.

Effects of plasma on Au_CR antibacterial activity

To determine its stability in plasma, Au_CR (final concentration 10 mg/mL) was mixed with 100% human plasma at 37 °C for 0, 0.5, 1, 2, 4, 6, 8, 10, 18, and 24 h, respectively. Residual antibacterial activity of the samples at each incubation time point was evaluated by measuring their MICs, as described above. The assay using human plasma samples were approved by the Institutional Review Board at the Kunming Institute of Zoology (KIZRKX-2021-XZ-003).

Animals

Female and male C57BL/6 mice (6–8 weeks old, 20-22 g) were used for all *in vivo* experiments. Mice were obtained from the Kunming Medical University, Yunnan, China. All mouse experiments and handling procedures were approved by and followed the guidelines of the Animal Care and Use Committee of the Kunming Institute of Zoology, Chinese Academy of Sciences (SMKX-2020023).

Pharmacokinetics and biodistribution study

Pharmacokinetics and biodistribution studies were performed on healthy female C57BL/6 mice (~20 g). The animals received an intravenous (i.v.) injection of Au_CR (Au dose 10 mg/kg), with blood samples then collected at 5 min and at 1, 3, 5,

24, and 48 h. The animals were sacrificed at 48 h and various organs, including the heart, liver, spleen, lungs, and kidneys, were collected. The blood and tissue samples were lyophilized, mashed, and digested in aqua regia. After digestion, the mixture was diluted with H_2O and precipitated tissue debris was removed by centrifugation at 10 000 rpm at 4 °C for 5 min. The Au content in the supernatant was measured by ICP-mass spectrometry (MS). Absolute Au content was expressed as μg/mL in blood or μg/g in tissue (~1.4 mL of blood was assumed for ~20-g mice). The pharmacokinetics data were fitted in a noncompartmental model using PKSolver software[22].

Acute toxicity of Au_CR *in vivo*

To determine the acute toxicity of Au_CR *in vivo*, female C57 mice (6–8 weeks old) were administrated via i.v. injection with a single dose of Au_CR or vancomycin at 20–40 mg/kg. After injection, mice (n = 10) were visually inspected for signs of toxicity three times a day for 96 h. Toxicity was rated based on the following observations: ruffled fur and poor motility = mild signs; hutching, very ruffled fur and complete immobility even under stimulation = manifest signs.

Survival experiments

In the first set of experiments, female C57BL/6 mice (n = 10) were intravenously inoculated with an inoculum of 1.6×10^9 CFU of *S. aureus* Z in 100 μL of sterile saline. Treatment with Au_CR (0.25, 0.5, and 1 mg/kg) and vancomycin (1 mg/kg) was performed (via i.v. injection) at 1 and 6 h after inoculation. In the second set of experiments, female C57BL/6 mice (n = 10) were first intraperitoneally injected with 5×10^8 CFU of *S. aureus* Z in 100 μL of sterile saline, followed by intraperitoneal (i.p.) administration of Au_CR (1, 2, and 4 mg/kg) and vancomycin (4 mg/kg) at 1 and 6 h after infection. The mice were observed 2-3 times each day, and the survival

rate was recorded for 72 h.

Effects of Au_CR on *S. aureus* lung disease

Female C57BL/6 mice (n = 6) were lightly anesthetized with inhaled isoflurane (RWD Life Science Co, Ltd, China) and an inoculum of 2×10^8 CFU of *S. aureus* Z in 20 μL of sterile saline was administered intranasally. Control mice were inoculated with 20 μL of saline. At 2 h post bacterial inoculation, the mice were administered (via i.v. injection) with increasing concentrations of Au_CR (1, 2, and 4 mg/kg) to test for dose dependence, with vancomycin (2 and 4 mg/kg) used as the control. At 12 h post treatment, mice were sacrificed via cervical dislocation and lungs were harvested and homogenized in 1 mL of PBS with a hand tissue grinder. Ten-fold serial dilutions of the homogenates at equal volumes were plated on LB agar plates at 37 °C. The CFUs were counted after 24 h. For histopathological analysis, lung sections were fixed in 4% paraformaldehyde, embedded in paraffin, and stained with hematoxylin & eosin (H&E).

***S. aureus*-induced bacteremia model**

Dissemination of *S. aureus* to target organs was evaluated in the *S. aureus*-induced bacteremia model. In brief, 100 μL of *S. aureus* Z suspension (1×10^9 CFU) was administered by i.p. injection into female C57BL/6 mice (n = 6). At 2 h after inoculation, Au_CR (1, 2, and 4 mg/kg) and vancomycin (2 and 4 mg/kg) were administered (via i.p. injection) into mice to assess their therapeutic effects. To evaluate bacterial dissemination to target organs, mice were sacrificed at 4 h post bacterial inoculation, and blood was collected via retro-orbital bleeding for cytokine evaluation. The spleen, liver, and lungs were also harvested. Blood was centrifuged at 2 000 rpm at 4 °C for 10 min to collect plasma. Cytokine levels of interleukin (IL)-1β, IL-6, IL-10, tumor necrosis factor (TNF)-α, monocyte chemotactic protein (MCP)-1,

and interferon (IFN)-γ in plasma were evaluated using standard ELISA kits (R&D systems, USA) following the manufacture's guidelines. The organs were homogenized on ice. Following 10-fold serial dilution in PBS, the homogenates were plated on LB agar plates and CFUs were determined. The organs were also used for histopathological analysis to determine the infiltration of inflammatory cells.

Statistical analysis

Differences in mean values among different groups were assessed, with results expressed as mean ± standard deviation (SD). Kolmogorov-Smirnov test was used in the analysis of normal distribution, and data were then analyzed using 1-way ANOVA, or 2-way ANOVA in case of measuring the effects of 2 factors simultaneously, with *post hoc* Dunnett or Bonferroni adjustment for p values. Data were analyzed using Prism 6.0 (Graphpad Software). Differences were considered significant at $p < 0.05$.

Supplemental Figures and Figure legends

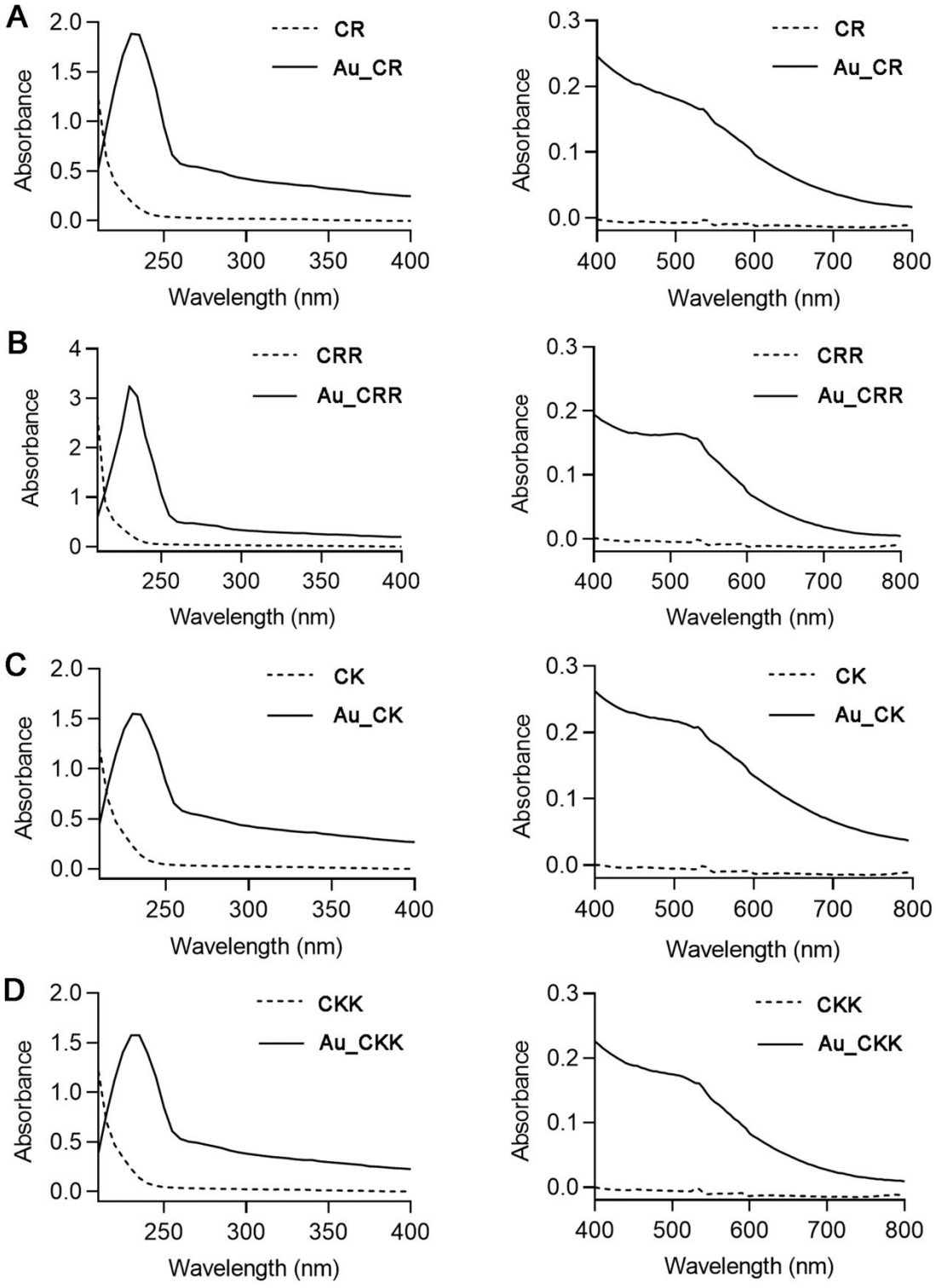

Fig. S1. UV-Vis spectra of short peptides (CR (A), CRR (B), CK (C), and CKK (D)) and short peptide-gold NPs. Data show scanning results within different wave length ranges.

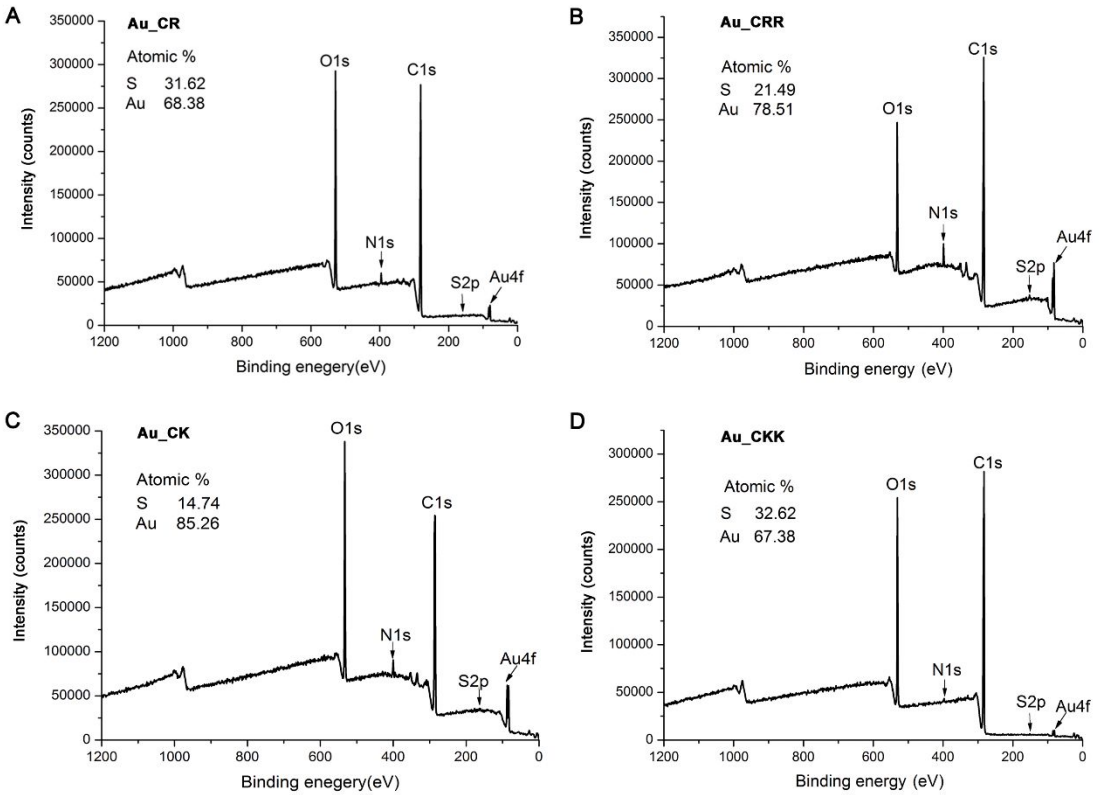

Fig. S2. XPS graphs of atomic % of S and Au in Au_CR (A), Au_CRR (B), Au_CK (C), and Au_CKK (D).

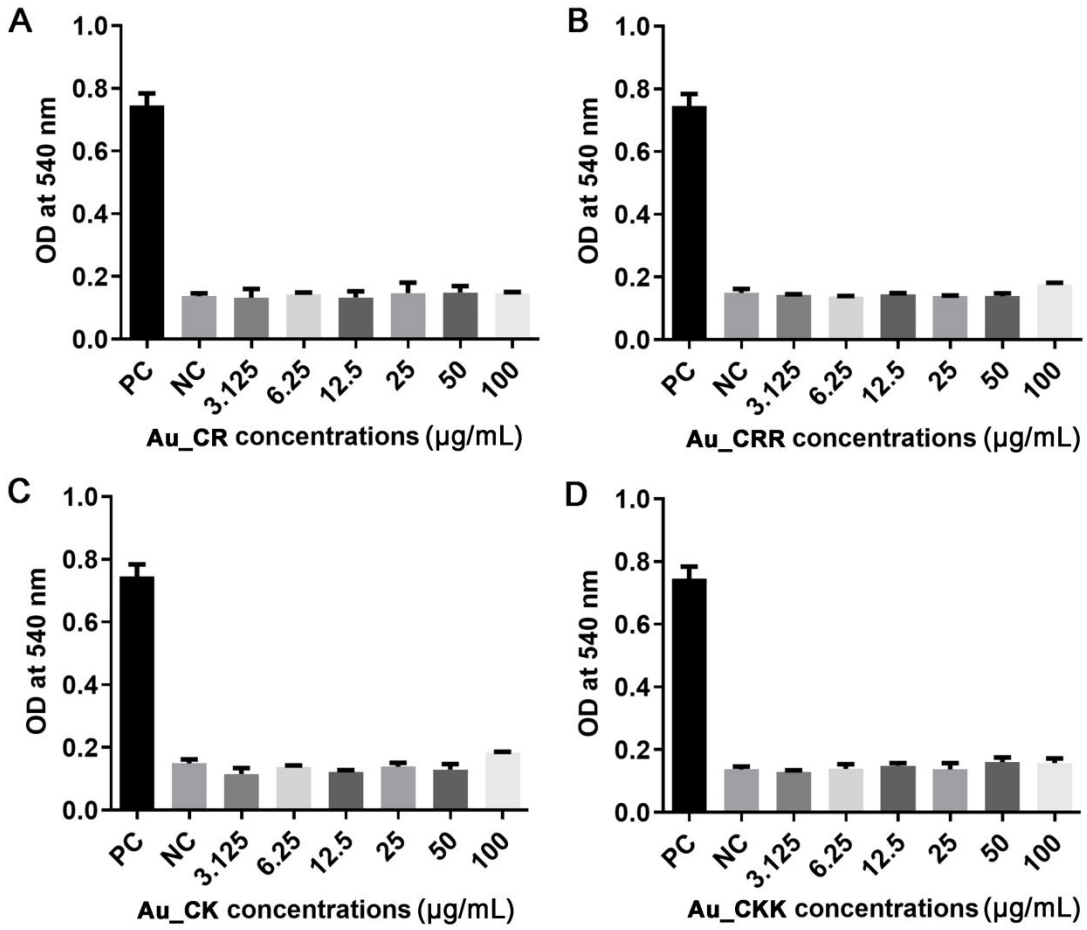

Fig. S3. Hemolytic activity of short peptide-gold nanoparticles on human erythrocytes. Potential hemolysis of Au_CR (A), Au_CRR (B), Au_CK (C), and Au_CKK (D) on human erythrocytes. Sterile PBS and 1% (v/v) Triton X-100 were used as negative (NC) and positive (PC) controls, respectively. Data represent mean ± SD of three independent experiments.

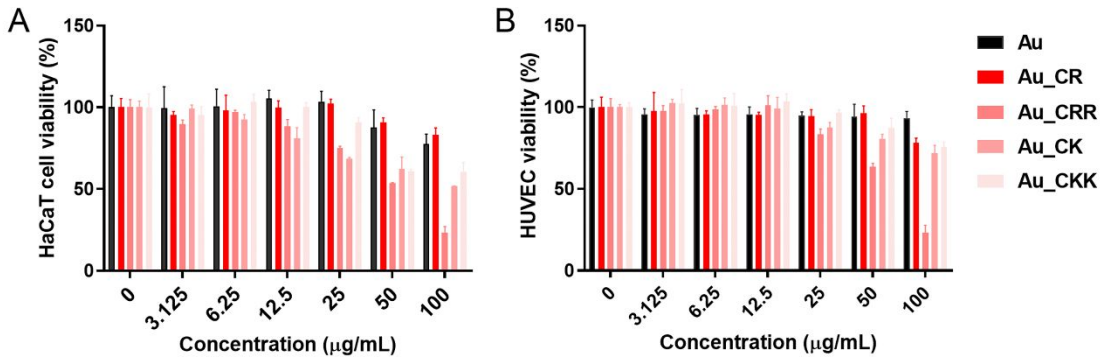

Fig. S4. Cytotoxicity of short peptide-gold nanoparticles. Potential toxicity of Au_CR, Au_CRR, Au_CK, and Au_CKK (0–100 μg/mL) on human HaCaT keratinocytes (A) and human umbilical vein endothelial cells (HUVECs) (B). Data represent mean ± SD of three individual experiments.

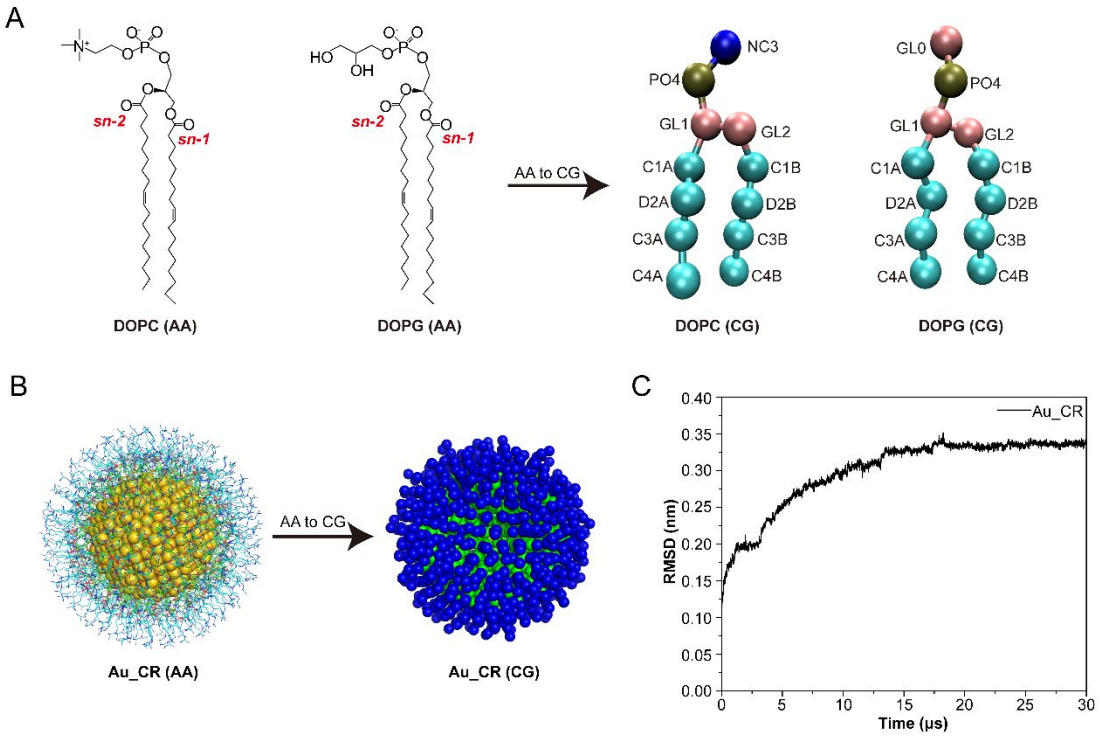

Fig. S5. CGMD simulation models and RMSD results. (A) All-atom (AA) and coarse-grained (CG) models of phospholipids DOPC and DOPG. The headgroups of DOPC and DOPG were colored in blue and pink, respectively. The PO4 beads were shown as tan color. The hydrophobic tails were in cyan and the glycerol beads were in pink. (B) All-atom (AA) and coarse-grained (CG) models of Au_CR particle. The gold atoms were shown as yellow spheres and CR peptides were shown as cyan lines for Cys and green lines for Arg residues. (C) The RMSD curve of Au_CR during MD simulations.

Parameter	Unit	Value
Lambda_z	1/h	0.0397454
t1/2	h	17.468281
Tmax	h	0.0833
Cmax	ng/ml	14.923163
C0	ng/ml	15.22305
Clast_obs/Cmax		0.1308142
AUC 0-t	ng/ml*h	267.09047
AUC 0-inf_obs	ng/ml*h	316.10525
AUC 0-t/0-inf_obs		0.843778
AUMC 0-inf_obs	ng/ml*h^2	7378.7052
MRT 0-inf_obs	h	23.444236
Vz_obs	(μg)/(ng/ml)	16.069954
Cl_obs	(μg)/(ng/ml)/h	0.6358389
Vss_obs	(μg)/(ng/ml)	14.974498

Fig. S6. Pharmacokinetic parameters analyzed by PKSolver of Au_CR via intravenous injection at Au dose of 10 mg/kg.

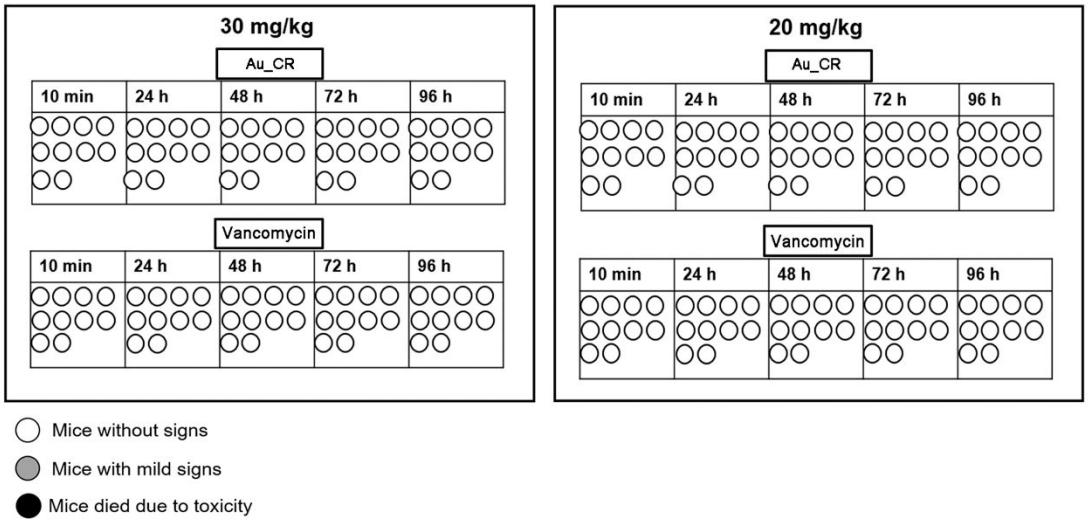

Fig. S7. *In vivo* acute toxicity of Au_CR and vancomycin. Female C57 mice (n = 10 mice/group) were administered (via i.v. injection) with a single dose of Au_CR or vancomycin at 20 and 30 mg/kg and monitored for 96 h. Circles each represent one mouse and toxicity score is indicated by different shading, as outlined in legend.

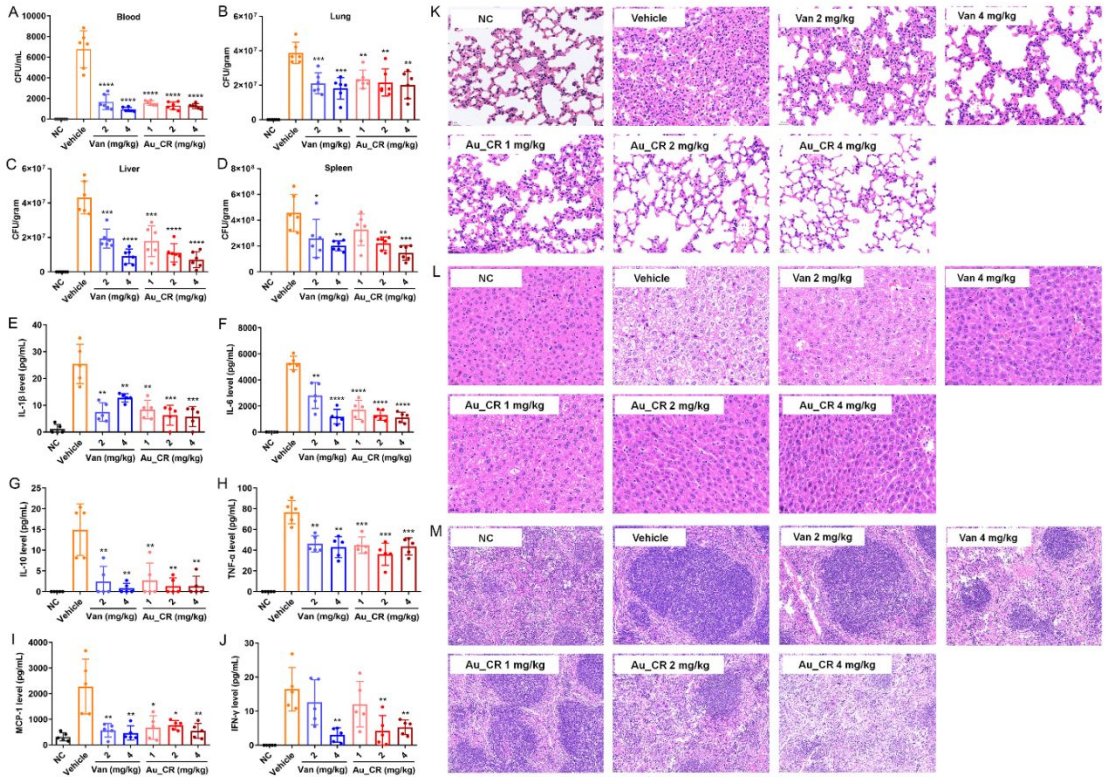

Fig. S8. Au_CR suppresses dissemination of *S. aureus* and inflammation. Mice (n = 6) were i.p. injected with *S. aureus*, followed by i.p injection of Au_CR (1, 2, 4 mg/kg) and vancomycin (2 and 4 mg/kg), or vehicle (saline). Bacterial burden was determined in blood (A), lung (B), liver (C), and spleen (D). (E-J) Plasma levels of IL-1β, IL-6, IL-10, TNF-α, MCP-1, and IFN-γ by ELISA. Representative histopathological images of lung (K), liver (L), and spleen (M) sections with H&E staining are shown. Mouse model experiments were repeated twice. NC: normal healthy mice; vehicle: sterile saline. *$p < 0.05$, **$p < 0.01$, ***$p < 0.001$, and ****$p < 0.0001$, two-way ANOVA with Dunnett *post hoc* test compared with vehicle group (sterile saline).

Supplemental Tables

Table S1. Components of NPs and surface charges in water at 25 °C.

	Molar ratio of oligopeptide to Au in NPs	Au atoms per NP	Oligopeptides per NP	Zeta potential (mV)
Au_CR	0.46:1	829	383	24.4 ± 1.4
Au_CRR	0.27:1	1661	448	16.0 ± 1.5
Au_CK	0.17:1	526	91	8.8 ± 1.5
Au_CKK	0.48:1	845	406	14.3 ± 2.2

Table S2. MICs of test samples against different *S. aureus* strains.

		MICs																		
		ATCC 2592	1184-1	1184-2	21441-1	21441-2	22082-1	22082-2	22082-3	1519-1	1519-2	8310	9431	11268	15775	11	31	32	51	52	Z
Au_CR	Au weight (μg/mL)	1.56	2.34	2.34	2.34	2.34	1.56	2.34	2.34	1.56	2.34	2.34	2.34	2.34	4.69	2.34	2.34	2.34	2.34	4.69	2.34
	NP molar (μM)	0.01	0.01	0.01	0.01	0.01	0.01	0.01	0.01	0.01	0.01	0.01	0.01	0.01	0.03	0.01	0.01	0.01	0.01	0.03	0.01
	CR molar (μM)	3.66	5.49	5.49	5.49	5.49	3.66	5.49	5.49	3.66	5.49	5.49	5.49	5.49	10.98	5.49	5.49	5.49	5.49	10.98	5.49
Au_CRR	Au weight (μg/mL)	6.25	9.38	6.25	9.38	6.25	6.25	6.25	6.25	6.25	6.25	9.38	12.50	9.38	12.50	6.25	6.25	6.25	6.25	6.25	6.25
	NP molar (μM)	0.02	0.03	0.02	0.03	0.02	0.02	0.02	0.02	0.02	0.02	0.03	0.04	0.03	0.04	0.02	0.02	0.02	0.02	0.02	0.02
	CRR molar (μM)	8.56	12.84	8.56	12.84	8.56	8.56	8.56	8.56	8.56	8.56	12.84	17.11	12.84	17.11	8.56	8.56	8.56	8.56	8.56	8.56
Au_CK	Au weight (μg/mL)	25.00	12.50	25.00	25.00	25.00	18.75	25.00	25.00	12.50	25.00	37.50	25.00	25.00	25.00	12.50	12.50	12.50	18.75	18.75	25.00
	NP molar (μM)	0.24	0.12	0.24	0.24	0.24	0.18	0.24	0.24	0.12	0.24	0.36	0.24	0.24	0.24	0.12	0.12	0.12	0.18	0.18	0.24
	CK molar (μM)	21.95	10.98	21.95	21.95	21.95	16.46	21.95	21.95	10.98	21.95	32.93	21.95	21.95	21.95	10.98	10.98	10.98	16.46	16.46	21.95
Au_CKK	Au weight (μg/mL)	6.25	6.25	6.25	9.38	6.25	6.25	6.25	6.25	6.25	6.25	9.38	9.38	6.25	12.50	6.25	6.25	6.25	6.25	6.25	6.25
	NP molar (μM)	0.04	0.04	0.04	0.06	0.04	0.04	0.04	0.04	0.04	0.04	0.06	0.06	0.04	0.08	0.04	0.04	0.04	0.04	0.04	0.04
	CKK molar (μM)	15.24	15.24	15.24	22.88	15.24	15.24	15.24	15.24	15.24	15.24	22.88	22.88	15.24	30.49	15.24	15.24	15.24	15.24	15.24	15.24
CR, CRR, CK, or CKK	Molar (μM)	> 200	> 200	> 200	> 200	> 200	> 200	> 200	> 200	> 200	> 200	> 200	> 200	> 200	> 200	> 200	> 200	> 200	> 200	> 200	> 200
Methicillin	Weight (μg/ml)	0.59	0.59	0.59	0.59	2.34	0.59	0.59	1.56	0.59	0.59	0.59	0.59	2.34	2.34	9.38	9.38	9.38	18.75	18.75	> 200
	Molar (μM)	1.46	1.46	1.46	1.46	5.79	1.46	1.46	3.86	1.46	1.46	1.46	1.46	5.79	5.79	23.25	23.25	23.25	46.50	46.50	> 495.79
Vancomycin	Weight (μg/ml)	1.56	1.17	1.17	1.17	1.17	1.17	1.17	1.56	1.17	1.17	1.17	1.17	1.17	1.17	1.17	2.34	2.34	2.34	2.34	1.17
	Molar (μM)	1.08	0.81	0.81	0.81	0.81	0.81	0.81	1.08	0.81	0.81	0.81	0.81	0.81	0.81	0.81	1.62	1.62	1.62	1.62	0.81

Concentrations represent mean values of three independent experiments. Strains of *S. aureus* 1184-1, 1184-2, 21441-1, 21441-2, 22081-1, 22082-2, 22082-3, 1519-1, 1519-2, 8310, 9431, 11268, 15775, 11, 31, 32, 51, 52, and Z were clinically isolated.

Table S3. Au_CR's antibacterial activity in plasma.

	Au_CR									
Time (h)	0	0.5	1	2	4	6	8	10	18	24
MIC (μg/mL)	1.56	1.56	1.56	1.56	1.56	1.56	1.56	1.56	1.56	1.56

Au_CR was first incubated with human plasma (final concentration 100 μg/mL) for 1–24 h. After incubation, MICs of plasma containing Au_CR against *S. aureus* ATCC2592 were determined. Data represent mean values of three independent experiments.

Supplementary References

1 Zhao, Y. *et al.* Small molecule-capped gold nanoparticles as potent antibacterial agents that target Gram-negative bacteria. *Journal of the American Chemical Society* **132**, 12349-12356, doi:10.1021/ja1028843 (2010).

2 Mwangi, J. *et al.* The antimicrobial peptide ZY4 combats multidrug-resistant Pseudomonas aeruginosa and Acinetobacter baumannii infection. *Proceedings of the National Academy of Sciences of the United States of America* **116**, 26516-26522, doi:10.1073/pnas.1909585117 (2019).

3 Omardien, S. *et al.* Bactericidal activity of amphipathic cationic antimicrobial peptides involves altering the membrane fluidity when interacting with the phospholipid bilayer. *Biochimica et biophysica acta. Biomembranes* **1860**, 2404-2415, doi:10.1016/j.bbamem.2018.06.004 (2018).

4 Abraham, M. J. *et al.* GROMACS: High performance molecular simulations through multi-level parallelism from laptops to supercomputers. *SoftwareX* **1-2**, 19-25, doi:10.1016/j.softx.2015.06.001 (2015).

5 Marrink, S. J., Risselada, H. J., Yefimov, S., Tieleman, D. P. & de Vries, A. H. The MARTINI Force Field: Coarse Grained Model for Biomolecular Simulations. *The Journal of Physical Chemistry B* **111**, 7812-7824, doi:10.1021/jp071097f (2007).

6 Vardeman, C. F., II, Stocker, K. M. & Gezelter, J. D. The Langevin Hull: Constant Pressure and Temperature Dynamics for Nonperiodic Systems. *Journal of Chemical Theory and Computation* **7**, 834-842, doi:10.1021/ct100670m (2011).

7 Martínez, L., Andrade, R., Birgin, E. G. & Martínez, J. M. PACKMOL: A package for building initial configurations for molecular dynamics simulations. *Journal of Computational Chemistry* **30**, 2157-2164, doi:10.1002/jcc.21224 (2009).

8 Hermann, K. in *Crystallography and Surface Structure* 265-266 (2011).

9 Heinz, H., Vaia, R. A., Farmer, B. L. & Naik, R. R. Accurate Simulation of Surfaces and Interfaces of Face-Centered Cubic Metals Using 12−6 and 9−6 Lennard-Jones Potentials. *The Journal of Physical Chemistry C* **112**, 17281-17290, doi:10.1021/jp801931d (2008).

10 Heinz, H., Lin, T.-J., Kishore Mishra, R. & Emami, F. S. Thermodynamically Consistent Force Fields for the Assembly of Inorganic, Organic, and Biological Nanostructures: The INTERFACE Force Field. *Langmuir* **29**, 1754-1765, doi:10.1021/la3038846 (2013).

11 Ganewatta, M. S. *et al.* Bio-inspired resin acid-derived materials as anti-bacterial resistance agents with unexpected activities. *Chemical Science* **5**, 2011-2016, doi:10.1039/C4SC00034J (2014).

12 Kim, W. *et al.* A selective membrane-targeting repurposed antibiotic with activity against persistent methicillin-resistant Staphylococcus aureus. *Proceedings of the National Academy of Sciences* **116**, 16529-16534, doi:10.1073/pnas.1904700116 (2019).

13 Wassenaar, T. A., Ingólfsson, H. I., Böckmann, R. A., Tieleman, D. P. & Marrink, S. J. Computational Lipidomics with insane: A Versatile Tool for Generating Custom Membranes for Molecular Simulations. *Journal of Chemical Theory and Computation* **11**, 2144-2155, doi:10.1021/acs.jctc.5b00209 (2015).
14 Marrink, S. J., de Vries, A. H. & Mark, A. E. Coarse Grained Model for Semiquantitative Lipid Simulations. *The Journal of Physical Chemistry B* **108**, 750-760, doi:10.1021/jp036508g (2004).
15 Bussi, G., Donadio, D. & Parrinello, M. Canonical sampling through velocity rescaling. *The Journal of Chemical Physics* **126**, 014101, doi:10.1063/1.2408420 (2007).
16 Berendsen, H. J. C., Postma, J. P. M., van Gunsteren, W. F., DiNola, A. & Haak, J. R. Molecular dynamics with coupling to an external bath. *The Journal of Chemical Physics* **81**, 3684-3690, doi:10.1063/1.448118 (1984).
17 Darden, T., York, D. & Pedersen, L. Particle mesh Ewald: An N·log(N) method for Ewald sums in large systems. *The Journal of Chemical Physics* **98**, 10089-10092, doi:10.1063/1.464397 (1993).
18 Parrinello, M. & Rahman, A. Polymorphic transitions in single crystals: A new molecular dynamics method. *Journal of Applied Physics* **52**, 7182-7190, doi:10.1063/1.328693 (1981).
19 Humphrey, W., Dalke, A. & Schulten, K. VMD: Visual molecular dynamics. *Journal of Molecular Graphics* **14**, 33-38, doi:10.1016/0263-7855(96)00018-5 (1996).
20 Schrodinger, LLC. *The PyMOL Molecular Graphics System, Version 1.8* (2015).
21 Jiang, X. *et al.* Nanomolar LL-37 induces permeability of a biomimetic mitochondrial membrane. *Nanoscale* **14**, 17654-17660, doi:10.1039/d2nr05409d (2022).
22 Zhang, Y., Huo, M., Zhou, J. & Xie, S. PKSolver: An add-in program for pharmacokinetic and pharmacodynamic data analysis in Microsoft Excel. *Computer methods and programs in biomedicine* **99**, 306-314, doi:10.1016/j.cmpb.2010.01.007 (2010).